An occurrence of radially-symmetric sedimentary structures in the basal Ediacaran cap dolostone (Keilberg Member) of the Otavi Group

CROCKFORD, P.W.[1,2], MEHRA, A.[3,4], DOMACK, E.[5,a], HOFFMAN, P.F.[2,6]

[1]*Department of Earth and Planetary Sciences, Weizmann Institute of Science Rehovot 76100 Israel. email: peter.crockford@weizmann.ac.il*
[2]*Department of Earth and Planetary Sciences, Harvard University, Cambridge MA 02138, USA*
[3]*Department of Geoscience, Princeton University, Princeton NJ 08544, USA*
[4]*Department of Earth Sciences, Dartmouth College, Hanover NH 03755, USA*
[5]*College of Marine Science, University of South Florida, St Petersburg FL 33701, USA*
[6]*School of Earth and Ocean Sciences, University of Victoria, Victoria BC V8W 2Y2, Canada*
[a]*Deceased*

May 26, 2021

This is a non-peer reviewed preprint submitted to EarthArXiv. The manuscript is currently in review for publication in Communications of the Geological Survey of Namibia. Subsequent versions of this paper may have slightly different content.

Corresponding Author: peter.crockford@weizmann.ac.il

An occurrence of radially-symmetric sedimentary structures in the basal Ediacaran cap dolostone (Keilberg Member) of the Otavi Group

CROCKFORD, P.W.[1,2], MEHRA, A.[3,4], DOMACK, E.[5,a], HOFFMAN, P.F.[2,6]

[1]*Department of Earth and Planetary Sciences, Weizmann Institute of Science Rehovot 76100 Israel. email: peter.crockford@weizmann.ac.il*
[2]*Department of Earth and Planetary Sciences, Harvard University, Cambridge MA 02138, USA*
[3]*Department of Geoscience, Princeton University, Princeton NJ 08544, USA*
[4]*Department of Earth Sciences, Dartmouth College, Hanover NH 03755, USA*
[5]*College of Marine Science, University of South Florida, St Petersburg FL 33701, USA*
[6]*School of Earth and Ocean Sciences, University of Victoria, Victoria BC V8W 2Y2, Canada*
[a]*Deceased*

Abstract: Snowball Earth cap carbonate sequences provide an archive of what are likely the most dramatic climate transitions in all of Earth history. One approach to gain insight into these events is the detailed observation of sedimentary structures within these post-glacial units. Here, we report on newly discovered radially-symmetric sedimentary structures within the Keilberg Member post-Marinoan 'cap dolostone' from the Otavi Group of northwest Namibia. We describe the local expression of over 60 decimeter-scale cymbal or disc structures from a single location. We interpret these features, which we name Zildjian structures, to be of likely abiotic origin. Through morphological comparisons, we suggest that Zildjian structures are most similar to *Astropolithon*, a pseudofossil which formed as a result of fluid or gas expulsion.

Keywords: Ediacaran; Marinoan; Neoproterozoic; Snowball Earth; Keilberg; Cap Carbonate; Pseudofossil; Discoidal structures; Disc; Cymbal; *Astropolithon*

Introduction

Persuasive geological and geochemical evidence suggests that the Neoproterozoic Era was punctuated by a pair of 'Snowball Earth' glaciations—the Marinoan (646 +/- 5 to 635 Ma; Kendall *et al.* 2006; Prave *et al.* 2016; Condon *et al.* 2005) and Sturtian (717 to 661 Ma; Macdonald *et al.* 2010; MacLennan *et al.* 2017; Rooney *et al.* 2014)—during which time the oceans were covered from pole to pole by dynamic ice sheets (Kirshvink 1992; Hoffman & Schrag, 2002; Hoffman *et al.* 2017; Hoffman *et al. in press*). The transitions out of these extreme climate states are documented by so called 'cap dolostones', which (in the case of the Marinoan) are layers of organic-poor micro-clotted, pseudo-peloidal (also described as micropeloidal or dolopelarenite) dolomite overlying glacial deposits and glacial erosion surfaces. These post-glacial carbonates have been observed to range in thickness from 10s of centimetres to 100s of metres (Grotzinger & Knoll, 1995; Hoffman *et al.* 1998, 2011; Hoffman & Li 2009). Cap dolostones are found on virtually all palaeocontinents and palaeogeographic reconstructions place deposition typically at ≤ 50˚ palaeolatitude (Hoffman & Li, 2009). These units represent the transgressive systems tract (i.e., post-glacial flooding) of thick depositional sequences that may have formed because of prolonged subsidence in a slow sedimentation regime (Partin *et al.* 2016). Cap dolostones contain many unusual (and, in certain cases, enigmatic) sedimentological features, including tubestone stromatolites (Corsetti & Grotzinger, 2005), digitate and fanning barites (e.g., Bao *et al.* 2008; Crockford *et al.* 2016; 2018; 2019), trochoidal bedforms interpreted as giant wave ripples (Allen & Hoffman, 2005; Lamb *et al.* 2012), and sheet cracks filled with fibrous isopachous dolomite cement (Hoffman & Macdonald, 2010; also cf. Hoffman (2011) for an in-depth review of cap dolostone sedimentology). In fact, Marinoan cap dolostones are so distinctive in character and setting that they defined the base of the Ediacaran Period (Knoll *et al.* 2006) before their age and synchroneity were known radiometrically (Rooney *et al.* 2015; Zhou *et al.* 2019).

One way to gain new perspectives on cap dolostone depositional processes is through the careful accounting and analysis of sedimentary features within them. Such features—from millimetre-scale wave ripples to metre-scale microbial buildups and kilometre-scale mud volcanoes—represent a record of physical forcings that can be used to understand past environmental conditions (Hoffman & Macdonald, 2010; Lamb *et al.* 2012). With such analyses in mind, we present a description of decimetre-scale radially-symmetrical sedimentary cymbal-shaped structures that are located within the Keilberg Member cap dolostone from the Congo craton in modern day Namibia. Due to their size and shape, we call these cymbal-like structures "Zildjians", after Armenian-Turkish-American family of cymbal manufacturers since 1618.

Geological Setting

The focus of this study is the Keilberg Member of the Maieberg Formation (Hedberg, 1979; SACS, 1980; Hoffman & Halverson, 2008), which is the basal Ediacaran formation within the Otavi Group. The study site is located near the village of Omukutu on the upper Hoanib River east of Khowarib, in the Kunene Region, of northwest Namibia (S19˚17'20.04" E13˚54'5.4"; Fig. 1). At the study location, the Maieberg Fm. is exposed as sub-vertically dipping, slightly overturned beds that face to the west. The Keilberg Member documents the initial post-glacial transgression from the Marinoan glaciation (Hoffman *et al.* 1998, 2011; Hoffman *et al*. 2021) across northwest Namibia and correlates with other, globally distributed formations that record similar geological events (Hoffman *et al.* 2017). The Omukutu area is situated on the inner Otavi Group carbonate platform at the western sidewall of the Omarumba trough (Fig. 1), a broad shallow depression cut by south-southwestward-flowing Marinoan ice. In this location, the Keilberg Member directly overlies the glacial erosion surface, marked by scraps of lodgement tillite, and passes gradationally upwards into marly limestone rhythmite of the middle Maieberg Formation postglacial maximum-flooding interval. The Keilberg Member at Omukutu is ≈23 m thick. Regionally, sections within the Omarumba trough range between 10-20 m in thickness but outside of the trough can expand to between 30-100 m (Fig. 1).

Field observations

Sixty-one different Zildjian structures were recorded in the Omukutu area (Fig 2). Most structures were observed to be between 7.8 and 9.1 m above the base of the Keilberg Member, although several were also found at 11.2, 13.0 and 13.5 m above the base of the section (Table 1). The stratigraphic interval containing the Zildjian structures was deposited above 'tubestone' stromatolites (Corrsetti & Grotzinger, 2005) and is comprised of dolomitized micropeloidal grainstone (i.e. dolopelarenite) characterized by swaley low-angle cross-stratification (Fig. 1). The Zildjians were identified as concentric circular ridges and depressions (Fig. 2). As previously mentioned, in the Omukutu area, beds were slightly overturned. Therefore, field measurements of Zildjians were made on the undersides of the structures (Fig. 2). Although the preservation of Zildjian structures varied across the outcrop (i.e. due to differential weathering), we applied a consistent measurement scheme to document those instances that we were safely able to reach.

In total, we were able to study approximately half of the 61 observed structures (n = 35). In what follows, we present observations as if observing Zildjian structures from right-way-up in horizontal beds unless otherwise specified. For each Zildjian, we measured an outer rim diameter (D_1), an inner trough diameter (D_2), a central axial pit diameter (D_3), and the distance to the next closest Zildjian (from center to center; S), all parallel to bedding (Fig. 3C; Table 1). We also measured an overall vertical relief where the undersides of structures protrude down from the bedding plane (H) and stratigraphic height (Z), both normal to bedding (Fig. 3C; Table 1). These measurements yielded a mean D_1 of 0.29 m [range: 0.12-0.70 m; n=29]; a mean D_2 of 0.09 m [range: 0.04-0.14 m; n=33]; a mean D_3 of 0.045 m [range: 0.015-0.075 m; n=33]; a mean H of 0.023 m [range: 0.005-0.048 m; n=24]; and a mean S of 1.07 m [range: 0.33-2.63; n=14] (Table 1). As observed, none of the structures exhibited any markings radiating away from the axial pit. Such observations have been documented in a number of interpreted Ediacaran and Cryogenian circular fossil imprints (e.g., MacGabhann, 2007; Inglez *et al.* 2019; Burzinski *et al.* 2020). We note that many of the Zildjian structures displayed a slight depression beyond the D_1 perimeter, approaching, in some cases, one metre in diameter. This slight depression radiating away from the underside of the Zildjian structures implies a slight doming of the bedding plane (Fig. 2A). Together, these measurements depict a regularity of Zildjian dimensions as well as somewhat regular spacings between them.

Two weathered blocks of float provided cross-sectional views of the Zildjian structures (Fig. 3A & 3B), thereby allowing a more detailed description of their sedimentological characteristics. In these two samples, we observed regular laminations in grainstone parallel to the bedding plane away from the structures. Moving towards the center of the structure, laminations deflected downward, reaching an angle of ≈ 45 degrees. Further inward, laminations curved back up toward the axial zone of the structures. In the axial zone, in the lower portion of the structures, the laminations appeared to stop and were replaced by infill (likely micritic), which in one sample displayed convex layering (Fig. 3B & 3D). Tracing the axial zone further up, however, laminations do bridge across the structures (Fig. 3D). This finding is consistent with continued sedimentation that draped over the resulting Zildjian bedform. In cross-section, we observed that, when vertically tracing the axial zone downwards (~ 10 cm), D_2 and D_3 varied. A possibility for the vertical heterogeneity of inter-Zildjian widths is differential exposure (i.e. differences in where the bedding plane intersects with different Zildjians) rather than true size dissimilarities between structures.

Interpretation

In what follows, we compare the Zildjian structures to reported discoidal sedimentary features of both abiotic and biotic interpreted sedimentary origins. Specifically, we focus on some of the key features highlighted above: the regular spacing between the Zildjians, the dimensions of the structures, the partial destruction of laminations in the axial pit, and the slight doming outside of the D_1 diameter. We utilise these observations to consider a biological versus abiotic origin for these structures. We would like to note, however, that further research, utilizing analyses such as detailed petrography and/or microscopy, will be needed to conclusively rule out particular interpretations.

There are several instances of documented sedimentary features that are both morphologically similar to Zildjians and have inferred biological origins. Examples of such features include Ediacaran and Cryogenian discoidal fossils such as *Aspidella* (e.g. MacGabhann, 2007), rooting or frond structures (Luzhnaya & Ivantsov 2019), Cambrian medusae (e.g. Young & Hagadorn, 2010) or features formed via microbial mats. Importantly, slight outer doming analogous to what we observed in the case of the Zildjian structures beyond the D_1 diameter (see above), has not been described in any of these examples. Zildjian structures have a decimetre-scale range of outer rim diameters (i.e. from 0.12 to 0.7 m), which is considerably larger than the range of diameters reported for Ediacaran discoidal fauna imprints (maximum diameter of < 0.15 m, with many reported in the sub-cm range; MacGabhann, 2007; Inglez *et al.* 2019; Burzinski *et al.* 2020) or the frond-like Petalonamae *Ediacaria flindersi* Sprigg (outer diameter of < 0.02 m; see Luzhnaya & Ivantsov 2019) or so called 'scratch circles' (Jensen *et al.* 2018). While Cambrian medusoids can reach similar sizes to the Keilberg Zildjians (e.g. Young & Hagadorn, 2010), other morphological characteristics disprove such an affinity. In particular, the destruction of bedding in the axial pit rules out an interpretation of Zildjians as surficial impressions resulting from a dead medusa-like organism. Additionally, the observed regular spacing of Zildjians is inconsistent with the expected spatial distribution of a death assemblage of medusae (i.e. maximum concentration in local troughs, Hagadorn & Miller, 2011). While such regular spacing may be induced via holdfasts of fronds, again, the magnitude of relief of the Zildjians is unlike reported scratch circles and the size of these structures does not match reported imprints from frond-bearing organisms. The final possibility is that Zildjians formed as a direct result of microbial construction such as a stromatolite. A challenge to this interpretation is that Zildjians are of different scale and morphology of documented stromatolite occurrences of this age (e.g. James *et al.* 2001; Bosak *et al.* 2013). While some instances of slightly crinkly laminations (Fig. 3) away from the axial zone may conform to expectations of microbial laminite morphology, the spacing (i.e. a lack of lateral contact) of Zildjians and relief is very different from documented domal microbial laminite occurrences (e.g. Romero *et al.* 2020). In sum, the outer doming, size, vertical disruption, and regular spacing of the Keilberg Zildjian structures do not match those of previously reported

Neoproterozoic or early Cambrian fauna, flora or microbial structures. Therefore, the lack of overlap of these key observations motivates consideration of an abiotic origin.

If the Keilberg Zildjian structures are unlikely to be of biological origin, then what sort of processes led to their formation? The shape, size, axial pit and distribution of Zildjians are very different from discoidal features produced by diagenetic concretions (e.g. Schwid *et al.* 2021) but are similar to interpreted gas and fluid escape structures (Dionne, 1973; Lowe, 1975) such as sand volcanoes. In particular, the structures exhibit a striking morphological resemblance to the pseudofossil *Astropolithon*, which is characterised by positive convex relief, a central sediment plug, circular shape, and a diameter of several millimetres to tens of centimetres (Pickerill & Harris, 1979). *Astropolithon* has been documented elsewhere in time and space (e.g. Walter, 1972; Mount, 1993; Seilacher & Goldring, 1996; Seilacher *et al.* 2002; Hagadorn & Miller, 2011), but, in contrast to the Zildjian structures, have typically been reported in siliciclastic-dominated units. Indeed, this difference in host-lithology may be responsible for the spectacular preservation (i.e. clearly visible deformation of laminations in cross section) of Zildjian structures in the Omukutu area. Initially *Astropolithon* was interpreted to be a trace fossil by Dawson (1878) but later investigations noted how the pseudofossil bears the same characteristics as sand or mud volcanoes (Seilacher *et al.* 2002). Thus, *Astropolithon* are now considered to be genetically similar to those sedimentary structures, forming as a result of the expulsion of over-pressurized gases or fluids (contained within pore spaces) out of a breach in the sediment-water interface (Lowe, 1975; Pickerill & Harris, 1979). The only suggested distinction between sand or mud volcanoes and *Astropolithon* is the presence of a less permeable surface layer in the latter, which results in slight doming beyond the central vent or aperture (Seilacher *et al.* 2002). In the case of a Silurian example from the Kufra Basin (Seilacher *et al.* 2002), this less- permeable surface layer was suggested to be a ‘biomat’. A potential point of contrast between *Astropolithon* and the reported Zildjian structures here, are that no evidence for an organic-rich seal was found in our study location. That said, at this time we cannot rule out the possibility of a microbial mat acting as a seal or impermeable layer. Additionally, we note that rapid cementation of carbonate laminae may have had a similar sealing effect where deformation then occurred within partially lithified sediments. With these considerations in mind, we further explore the potential origins of Zildjian structures below.

If the Zildijian structures are indeed *Astropolithon*-like constructions, they formed because of either gas or fluid escape from sediments and, in turn, these physical events were likely triggered by either degradation of organic matter, seismic activity, or rapid sediment loading (Fig. 4). Multiple exposed horizons make selecting a definitive set and order of genetic events challenging. We first consider gas escape. A possible formation mechanism is the degradation of organic matter, which may have produced pockets of gases that pooled in place until sudden expulsion through beds. Previous work has suggested that 'balloon' structures in sands (Hilbert-Wolf *et al.* 2016) are a key feature of gas escape. However, such features are absent from our study area. Although a difference in host lithology may be responsible for the lack of balloon structures, their absence potentially supports fluid escape versus gas escape as the primary expulsion events resulting in Zildjian structures. A second potential piece of evidence in support of fluid escape is the upward deflection of beds into the axial pit; similar features have been shown in fluid-escape experiments conducted in siliciclastic sand and silt (e.g. Nichols *et al.* 1994). While there are many documented examples of fluidization structures with inferred relationships to seismicity, we did not observe, nor can we correlate, episodes of faulting or other physical indicators that would pinpoint a seismic trigger. Moreover, the appearance of the Keilberg Zildjians in multiple beds, as well as the possibility of the variation of the D_2 and D_3 diameters at the outcrop being caused by multiple expulsion episodes, appears to require a mechanism for repeated triggering. The combination of post-glacial sea level rise and glacial unloading could potentially produce seismic activity in the study area. However, further work is needed to identify and link such observations. An alternative possibility is that rapid loading may have been the underlying cause of the Keilberg Zildjians. Indeed, rapid sedimentation events have been suggested as the most common cause of fluid-escape structures in the sedimentary record (Lowe, 1975). However, this hypothesis is negated if fine mm-scale laminations in cross section require slower sedimentation. In sum, through morphological comparison Zildjians appear to bear the most similarity to *Astropolithon* and are likely the result of fluid or gas escape from sediments, however further work is warranted in order to constrain their origins at this time more precisely.

Conclusions

Here we have described a new sedimentary feature within post-Marinoan cap carbonate in the Omukutu area of Namibia. The features most closely resemble the pseudo fossil *Astropolithon* indicating fluid or gas expulsion and are therefore unlikely to be the result of a fossil imprint or direct microbial construction. At this time, further interpretation is challenging without detailed petrography, microscopy, and geochemical analyses, which are greatly encouraged in future work. Importantly, if such structures resulted from fluid escape, they may provide support for models of rapid cap dolostone sedimentation. The lack of prior reports of Zildjian structures, and their discovery in the Omukutu area within the most extensively studied Cryogenian field area that has been developed to date, is potentially due to their exposure in vertically dipping beds with well exposed bedding planes. Indeed, there may be many other roughly time-equivalent occurrences of Zildjians or similar structures within post-Marinoan strata and therefore further exploration is warranted.

Acknowledgements

The authors thank Adam Maloof and Shahar Hegyi for insightful conversations during the preparation of this manuscript and Alex De Moor for aiding in fieldwork. PWC would like to thank the Agouron Institute for post-doctoral funding during the preparation of this manuscript. AM acknowledges funding through the Dartmouth Neukom Fellowship Program.

References

Allen, P.A. & Hoffman, P.F. 2005. Extreme winds and waves in the aftermath of a Neoproterozoic glaciation. *Nature*, 433, 123-127. https://doi.org/10.1038/nature03176

Bao, H., Lyons, J.R. & Zhou, C. 2008. Triple oxygen isotope evidence for elevated CO2 levels after a Neoproterozoic glaciation. *Nature*, 453 (7194), 504-506. https://doi.org/10.1038/nature06959

Bosak, T., Mariotti, G., MacDonald, F.A., Perron, J.T. & Pruss, S.B. 2013. Microbial sedimentology of stromatolites in Neoproterozoic cap carbonates. *The Paleontological Society Papers*, 19, 51-76. DOI:10.1017/s1089332600002680

Burzynski, G., Dececchi, T.A., Narbonne, G.M. & Dalrymple, R.W. 2020. Cryogenian *Aspidella* from northwestern Canada. *Precambrian Research*, 336, 105507. https://doi.org/10.1016/j.precamres.2019.105507

Condon, D., Zhu, M., Bowring, S., Wang, W., Yang, A. & Jin, Y. 2005. U-Pb ages from the Neoproterozoic Doushantuo Formation, China. *Science*, 308 (5718), 95-98. DOI: 10.1126/science.1107765

Corsetti, F.A. & Grotzinger, J.P. 2005. Origin and significance of tube structures in Neoproterozoic post-glacial cap carbonates: example from Noonday Dolomite, Death Valley, United States. *Palaios*, 20 (4), 348-362. https://doi.org/10.2110/palo.2003.p03-96

Crockford, P.W., Cowie, B.R., Johnston, D.T., Hoffman, P.F., Sugiyama, I., Pellerin, A., Bui, T.H., Hayles, J., Halverson, G.P., Macdonald, F.A. & Wing, B.A. 2016. Triple oxygen and multiple sulfur isotope constraints on the evolution of the post-Marinoan sulfur cycle. *Earth and Planetary Science Letters*, 435, 74-83. https://doi.org/10.1016/j.epsl.2015.12.017

Crockford, P.W., Hodgskiss, M.S., Uhlein, G.J., Caxito, F., Hayles, J.A. & Halverson, G.P. 2018. Linking paleocontinents through triple oxygen isotope anomalies. *Geology*, 46 (2), 179-182. https://doi.org/10.1130/G39470.1

Crockford, P.W., Wing, B.A., Paytan, A., Hodgskiss, M.S., Mayfield, K.K., Hayles, J.A., Middleton, J.E., Ahm, A.S.C., Johnston, D.T., Caxito, F. and Uhlein, G., 2019. Barium-isotopic constraints on the origin of post-Marinoan barites. *Earth and Planetary Science Letters*, *519*, pp.234-244. https://doi.org/10.1016/j.epsl.2019.05.018

Dawson J. W. 1878. Supplement to the second edition of *Acadian Geology*. *In*: Acadian Geology, the geological structure, organic remains and mineral resources of Nova Scotia, New Brunswick and Prince Edward Island. 3rd Edition. MacMillan, London, 102 pp.

Dionne, J.C. 1973. Monroes; a type of so-called mud volcanoes in tidal flats. *Journal of Sedimentary Research*, 43 (3), 848-856.

Grotzinger, J.P. & Knoll, A.H. 1995. Anomalous carbonate precipitates; is the Precambrian the key to the Permian? *Palaios*, 10 (6), 578-596.

Hagadorn, J. & Miller, R. 2011. Hypothesized Cambrian medusae from Saint John, New Brunswick, reinterpreted as sedimentary structures. *Atlantic Geology*, 47, 66-80. doi: 10.4138/atlgeol.2011.002

Hedberg, R.M. 1979. Stratigraphy of the Ovamboland Basin, South West Africa. *University of Cape Town Precambrian Research Unit Bulletin*, 24, 325 p. and 6 map sheets scale 1:125,000.

Hilbert-Wolf, H.L., Roberts, E.M. & Simpson, E.L. 2016. New sedimentary structures in seismites from SW Tanzania: Evaluating gas- vs. water-escape mechanisms of soft-sediment deformation. *Sedimentary Geology*, 344, 253-262. https://doi.org/10.1016/j.sedgeo.2016.03.011

Hoffman, P.F. 2011. Strange bedfellows: glacial diamictite and cap carbonate from the Marinoan (635 Ma) glaciation in Namibia. *Sedimentology*, 58(1), 57-119. https://doi.org/10.1111/j.1365-3091.2010.01206.x

Hoffman, P.F., Abbot, D.S., Ashkenazy, Y., Benn, D.I., Brocks, J.J., Cohen, P.A., Cox, G.M., Creveling, J.R., Donnadieu, Y., Erwin, D.H. & Fairchild, I.J. 2017. Snowball Earth climate dynamics and Cryogenian geology-geobiology. *Science Advances*, 3 (11), p.e1600983. DOI: 10.1126/sciadv.1600983

Hoffman, P.F. & Halverson, G.P. 2008. Otavi Group of the western Northern Platform, the eastern Kaoko Zone and the western Northern Margin Zone. *In:* Miller, R. McG. (Ed.) *The Geology of Namibia, Volume 2.* Geological Survey of Namibia, 3, 13.69−13.136.

Hoffman, P.F., Halverson, G.P., Schrag, D., Higgins, J.A., Domack, E.W., Macdonald, F.A., Pruss, S.B., Blattler, C.L., Crockford, P.W., Hodgin, E.B., Bellefroid, E.J., Johnson, B.W., Hodgskiss, M.S.W., Lamothe, K.G., LoBianco, S.J.C., Busch, J.F., Howes, B.J., Greenman, J.W., Nelson, L.L. Snowballs in Africa: sectioning a long-lived Neoproterozoic carbonate platform and its bathyal foreslope (NW Namibia). *Earth Science Reviews* (*in press)* https://doi.org/10.1016/j.earscirev.2021.103616

Hoffman, P.F., Kaufman, A.J., Halverson, G.P. & Schrag, D.P. 1998. A Neoproterozoic snowball earth. *Science*, 281 (5381), 1342-1346. DOI: 10.1126/science.281.5381.1342

Hoffman, P.F. & Li, Z.X. 2009. A palaeogeographic context for Neoproterozoic glaciation. *Palaeogeography, Palaeoclimatology, Palaeoecology*, 277 (3-4), 158-172. https://doi.org/10.1016/j.palaeo.2009.03.013

Hoffman, P.F. & Macdonald, F.A. 2010. Sheet-crack cements and early regression in Marinoan (635 Ma) cap dolostones: Regional benchmarks of vanishing ice-sheets?. *Earth and Planetary Science Letters*, 300 (3-4), 374-384. https://doi.org/10.1016/j.epsl.2010.10.027

Hoffman, P.F. & Schrag, D.P. 2002. The snowball Earth hypothesis: testing the limits of global change. *Terra nova*, 14 (3), 129-155. https://doi.org/10.1046/j.1365-3121.2002.00408.x

Inglez, L., Warren, L.V., Okubo, J., Simões, M.G., Quaglio, F., Arrouy, M.J. & Netto, R.G. 2019. Discs and discord: The paleontological record of Ediacaran discoidal structures in the south American continent. *Journal of South American Earth Sciences*, 89, 319-336. https://doi.org/10.1016/j.jsames.2018.11.023

James, N.P., Narbonne, G.M. & Kyser, T.K. 2001. Late Neoproterozoic cap carbonates: Mackenzie Mountains, northwestern Canada: precipitation and global glacial meltdown. *Canadian Journal of Earth Sciences*, 38 (8), 1229-1262.

Jensen, S., Högström, A.E., Almond, J., Taylor, W.L., Meinhold, G., Høyberget, M.A.G.N.E., Ebbestad, J.O.R., Agić, H.E.D.A. & Palacios, T. 2018. Scratch circles from the Ediacaran and Cambrian of Arctic Norway and southern Africa, with a review of scratch circle occurrences. *Bulletin of Geosciences*, 93, pp. 287-304

Kendall, B., Creaser, R.A. & Selby, D. 2006. Re-Os geochronology of postglacial black shales in Australia: Constraints on the timing of "Sturtian" glaciation. *Geology*, 34 (9), 729-732. https://doi.org/10.1130/G22775.1

Kilner, B., Niocaill, C. & Brasier, M. 2005. Low-latitude glaciation in the Neoproterozoic of Oman. *Geology*, 33 (5), 413-416. https://doi.org/10.1130/G21227.1

Kirschvink, J.L. 1992. Late Proterozoic low-latitude global glaciation: the snowball Earth in *The Proterozoic Biosphere: A Multidisciplinary Study*, J. W. Schopf, C. Klein, D. Des Maris, Eds. (Cambridge Univ. Press, 1992), pp. 51–52.

Knoll, A., Walter, M., Narbonne, G. & Christie-Blick, N. 2006. The Ediacaran Period: a new addition to the geologic time scale. *Lethaia*, 39(1), 13-30. https://doi.org/10.1080/00241160500409223

Lamb, M.P., Fischer, W.W., Raub, T.D., Perron, J.T. & Myrow, P.M. 2012. Origin of giant wave ripples in snowball Earth cap carbonate. *Geology*, 40 (9), 827-830. https://doi.org/10.1130/G33093.1

Lowe, D.R. 1975. Water escape structures in coarse-grained sediments. *Sedimentology*, 22 (2), 157-204. https://doi.org/10.1111/j.1365-3091.1975.tb00290.x

Luzhnaya, E.A. & Ivantsov, A.Y. 2019. Skeletal Nets of the Ediacaran Fronds. *Paleontological Journal*, 53 (7), 667-675. https://doi.org/10.1134/S0031030119070050

MacGabhann, B.A. 2007. Discoidal fossils of the Ediacaran biota: a review of current understanding. *Geological Society, London, Special Publications*, 286 (1), 297-313. https://doi.org/10.1144/SP286.21

MacLennan, S., Park, Y., Swanson-Hysell, N., Maloof, A., Schoene, B., Gebreslassie, M., Antilla, E., Tesema, T., Alene, M. & Haileab, B. 2018. The arc of the Snowball: U-Pb dates constrain the Islay anomaly and the initiation of the Sturtian glaciation. *Geology*, 46 (6), 539-542. https://doi.org/10.1130/G40171.1

Mount, J.F. 1993. Formation of fluidization pipes during liquefaction: examples from the Uratanna Formation (Lower Cambrian), South Australia. *Sedimentology*, 40 (6), 1027-1037. https://doi.org/10.1111/j.1365-3091.1993.tb01378.x

Nichols, R.J., Sparks, R.S.J. & Wilson, C.J.N. 1994. Experimental studies of the fluidization of layered sediments and the formation of fluid escape structures. *Sedimentology*, 41 (2), 233-253. https://doi.org/10.1111/j.1365-3091.1994.tb01403.x

Partin, C.A. & Sadler, P.M. 2016. Slow net sediment accumulation sets snowball Earth apart from all younger glacial episodes. *Geology*, 44 (12), 1019-1022. https://doi.org/10.1130/G38350.1

Pickerill, R.K. & Harris, I.M. 1979. A reinterpretation of *Astropolithon hindii* Dawson 1878. *Journal of Sedimentary Research*, 49 (3), 1029-1036. https://doi.org/10.1306/212F78AB-2B24-11D7-8648000102C1865D

Prave, A.R., Condon, D.J., Hoffmann, K.H., Tapster, S. & Fallick, A.E. 2016. Duration and nature of the end-Cryogenian (Marinoan) glaciation. *Geology*, 44 (8), 631-634. https://doi.org/10.1130/G38089.1

Raub T. 2008. *Prolonged Deglaciation of "Snowball Earth*, Thesis, Yale University

Romero, G.R., Sanchez, E.A., Soares, J.L., Nogueira, A.C.R. & Fairchild, T.R. 2020. Waxing and waning of microbial laminites in the aftermath of the Marinoan glaciation at the margin of the Amazon Craton (Brazil). *Precambrian Research*, 348, p.105856. https://doi.org/10.1016/j.precamres.2020.105856

Rooney, A.D., Macdonald, F.A., Strauss, J.V., Dudás, F.Ö., Hallmann, C. & Selby, D. 2014. Re-Os geochronology and coupled Os-Sr isotope constraints on the Sturtian snowball Earth. *Proceedings of the National Academy of Sciences*, 111 (1), 51-56. https://doi.org/10.1073/pnas.1317266110

Rooney, A.D., Strauss, J.V., Brandon, A.D. & Macdonald, F.A. 2015. A Cryogenian chronology: Two long-lasting synchronous Neoproterozoic glaciations. *Geology*, 43 (5), 459-462. https://doi.org/10.1130/G36511.1

SACS (South African Committee for Stratigraphy) 1980. Damara Sequence. *In:* Kent, L.E. (Ed.) *Stratigraphy of South Africa Part 1: Lithostratigraphy of the Republic of South Africa, South West Africa/Namibia and the Republics of Bophuthatswana, Transkei and Venda*. Geological Survey of South Africa Handbook, 8, 415-438.

Seilacher, A. & Goldring, R. 1996. Class Psammocorallia (Coelenterata, Vendian-Ordovician): Recognition, systematics, and distribution. *GFF*, 118 (4), 207-216. https://doi.org/10.1080/11035899609546256

Seilacher, A., Lüning, S., Martin, M.A., Klitzsch, E., Khoja, A. & Craig, J. 2002. Ichnostratigraphic correlation of lower Palaeozoic clastics in the Kufra Basin (SE Libya). *Lethaia*, 35 (3), 257-262. https://doi.org/10.1111/j.1502-3931.2002.tb00083.x

Schwid, M.F., Xiao, S., Nolan, M.R. & An, Z. 2021. Differential Weathering of Diagenetic Concretions and the Formation of Neoproterozoic Annulated Discoidal Structures. *Palaios*, 36 (1), 15-27. https://doi.org/10.2110/palo.2020.018

Walter, M.R. 1972. Tectonically deformed sand volcanoes in a Precambrian greywacke, Northern Territory of Australia. *Journal of the Geological Society of Australia*, 18, 395-399. https://doi.org/10.1080/00167617208728777

Young, G.A. & Hagadorn, J.W. 2010. The fossil record of cnidarian medusae. *Palaeoworld*, 19 (3-4), 212-221. https://doi.org/10.1016/j.palwor.2010.09.014

Zhou, C., Huyskens, M.H., Lang, X., Xiao, S. & Yin, Q.Z. 2019. Calibrating the terminations of Cryogenian global glaciations. *Geology*, 47 (3), 251-254. https://doi.org/10.1130/G45719.1

Table and Figure Captions

Table 1. Dimensional data on cymbal-like structures in stratigraphic order (top to bottom). All measurements in metres: #, structure number; Z, stratigraphic height with respect to base of Keilberg Mb; D_1, disc outer diameter; D_2, inner rim diameter; D_3, axial pit diameter; H, overall vertical relief; S, distance to nearest structure at same horizon. Total thickness of Keilberg Member, 18.2 m. Base of tubestone stromatolite, 0.5-1.2 m; top of tubestone stromatolite, 6.5-9.4 m (with respect to the base of the Keilberg Mb). Remainder of Keilberg Member composed of laminated dolopelarenite with low-angle hummocky cross-stratification. D_1 average 0.296 m [0.12-0.70] n=29; D_2 average 0.093 m [0.04-0.14] n=33; D_3 average 0.0415 m [0.015-0.075] n=33; H average 0.231 m [0.010-0.048] n=24; S average 1.07 m [0.33-2.63] n=14.

Fig. 1. Geology and representative columnar section of the Keilberg Member in the study area. In the top centre map panel, the area bearing the Zildjians in the foreland thrust-fold belt of the Ediacaran Kaoko orogen is outlined by the white rectangle. Bedrock includes pre-orogenic carbonate formations of the Otavi Group (770-600 Ma) and synorogenic clastics of the Sesfontein Formation (Mulden Group). Glacigenic Chuos and Ghaub formations are too thin to show at this scale. The white rectangle is in the W-facing but E-dipping limb of an anticline in the hanging wall of a W-directed backthrust. Local topographic relief is 425 m relative to the Hoanib River, which has perennial flowing surface water in this area. A vehicle track (purple line) connects westward to Khowarib and eastward to Omukutu and Ombaatjie. The field campsite is indicated by a small yellow triangle. In the top right panel, a representative columnar section of Keilberg Member cap dolostone in the white rectangular area of the map panel and red rectangle of the cross section in the lower panel are presented. Numbered lithologic units: 1 - Ghaub Formation (Marinoan) carbonate diamictite inferred to be a lodgement tillite derived from underlying upper Ombaatjie Formation (left panel); 2 - low-angle cross-stratified dolopelarenite (peloid grainstone); 3 - tubestone stromatolite (Corsetti & Grotzinger, 2005); 4 - low-angle cross-stratified dolopelarenite with peloidal sand volcanoes at horizons indicated; 5 - thin planar-laminated dolomicrite with argillaceous partings increasing upward; 6 - marly calcite rhythmite. Stratigraphic height is in metres above the base of the Keilberg Member (0.0 m). In the lower cross section panel, selected Ombaatjie Fm sections are plotted from the OPz and IPz which outline the Omarumba trough. The insert map at the bottom of the panel shows relative section locations. Palaeotopography is reconstructed assuming as a datum when carbonate carbon isotope values from previous studies cross 0.0 per mil in cycle b7 (Hoffman *et al*. 2021), which, elsewhere, is supported by correlation of Keilberg Member thickness with stratigraphic height above this datum (Hoffman *et al*., 2021). The Omarumba trough has been inferred to be a subglacial bedrock trough formed via partial removal of b8 and b7 cycles via Marinoan glacial erosion (Hoffman *et al*. 2021). A legend is provided in the top left of the figure.

Fig. 2. Sedimentological expression of the undersides of Zildjian structures in overturned beds in the Omukutu area. (A) Bedding plane image of undersides of multiple Zildjian structures at the outcrop (ruler in images is in cm). Note that in (A) Zildjians are surround by a slight depression beyond D_1 diameter and that since beds are slightly overturned this suggests a doming of the bedding plane. (B-D) Three examples of Zildjian structures.

Fig. 3. Cross sectional view of Zildjian structures from two float samples. (A, B) Photos of two Zildjian cross sections of float samples in the Omukutu area. Note that photos are presented in interpreted stratigraphic up orientation and that the Bic crystal pen length (scale) is 14.9 cm. A cross sectional schematic provided in (C) where D_1 outer diameter, D_2 diameter at upper lip, D_3 diameter in axial pit, H synoptic height and S lateral spacing between discs is shown. (D) a zoomed in view of a portion of one of the Zildjian cross sections (denoted by the white dashed box in B) is presented where convex beds under the structure, destruction of laminations and traceable laminations across the structure are shown.

Fig. 4. Representation of possible Zildjian formation mechanisms. (A) Initial sedimentation; (B) triggering mechanisms; (C) deformation of beds; (D) Zildjian formation including a cross-sectional, plan and underside view of the structures. A scale is provided on the lower right of the figure.

#Z	D_1	D_2	D_3	H	S	
60	13.5	-	0.12	0.033	0.015	
62	13.0	0.70	0.08	0.07	0.03	
52	11.25	-	0.067	0.040	0.005	
17	9.1	0.40	0.08	0.035	0.014	
50	9.1	0.21	0.07	0.035		1.32
51	9.05	0.3	0.110	0.05	0.013	
2	8.7	0.20	0.11		0.016	2.63
3	8.7	0.28	0.07	0.040	0.018	0.84
10	8.7	-	0.04	0.015		
22	8.65	0.224	0.092	0.066		0.72
23	8.65	0.12	0.046	0.028		0.86
30	8.65					
31	8.65					
32	8.61	0.275	0.116	0.058	0.018	1.6
1	8.6	0.28	0.12	0.06	0.025	
19	8.55	0.28	0.07	0.051	0.03	0.76
20	8.55	0.26	0.12	0.072	0.048	0.52
21	8.55	0.20	0.078	0.055	0.014	
25	8.55	-	0.130	0.035		0.33
26	8.55	0.15	0.090	0.030		1.16
27	8.55	0.275	0.165	0.065	0.017	
29	8.55	0.190	0.080	0.050	0.015	1.33
18	8.3	0.26	0.07	0.05		
53	8.3	-	0.09	0.03		
6	8.25	0.50	0.09	0.04	0.023	1.03
7	8.25	0.46	0.11	0.04	0.032	
8	8.25	0.55	0.10	0.05	0.04	1.04
9	8.25	0.34	-	0.06	0.03	
11	8.25	0.40	0.04	0.03		
15	8.25	0.5	0.14	0.055	0.04	0.86
4	8.2	0.16	0.04	0.015	0.020	
24	8.2	0.270	0.140	0.030	0.010	
28	8.11	0.245	0.135	0.075	0.048	
5	7.8	0.20	0.08	0.051	0.013	
16	float	0.23	0.12	0.05		
61	float	0.12	0.06	0.03	0.02	

556

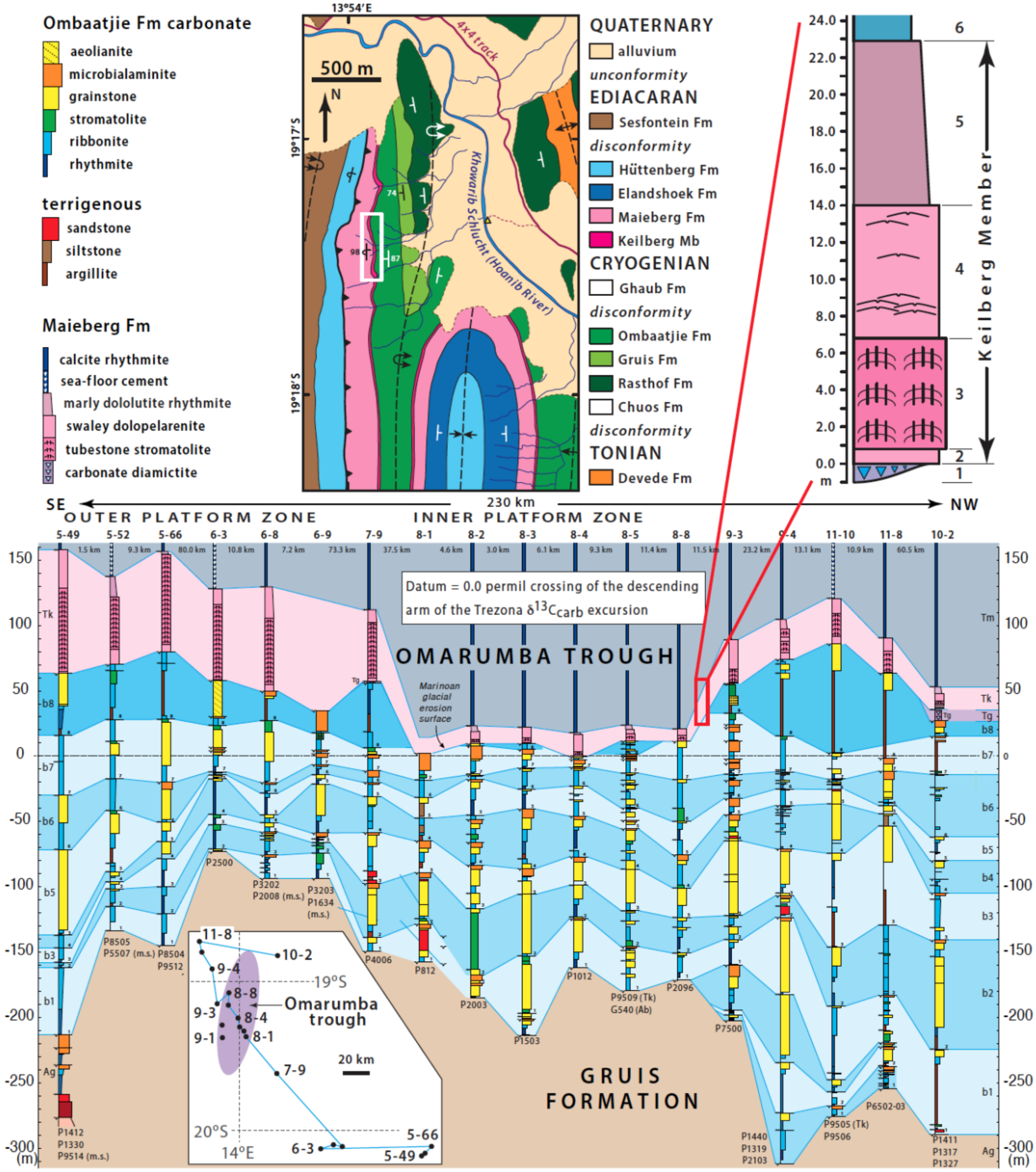

557

558

559

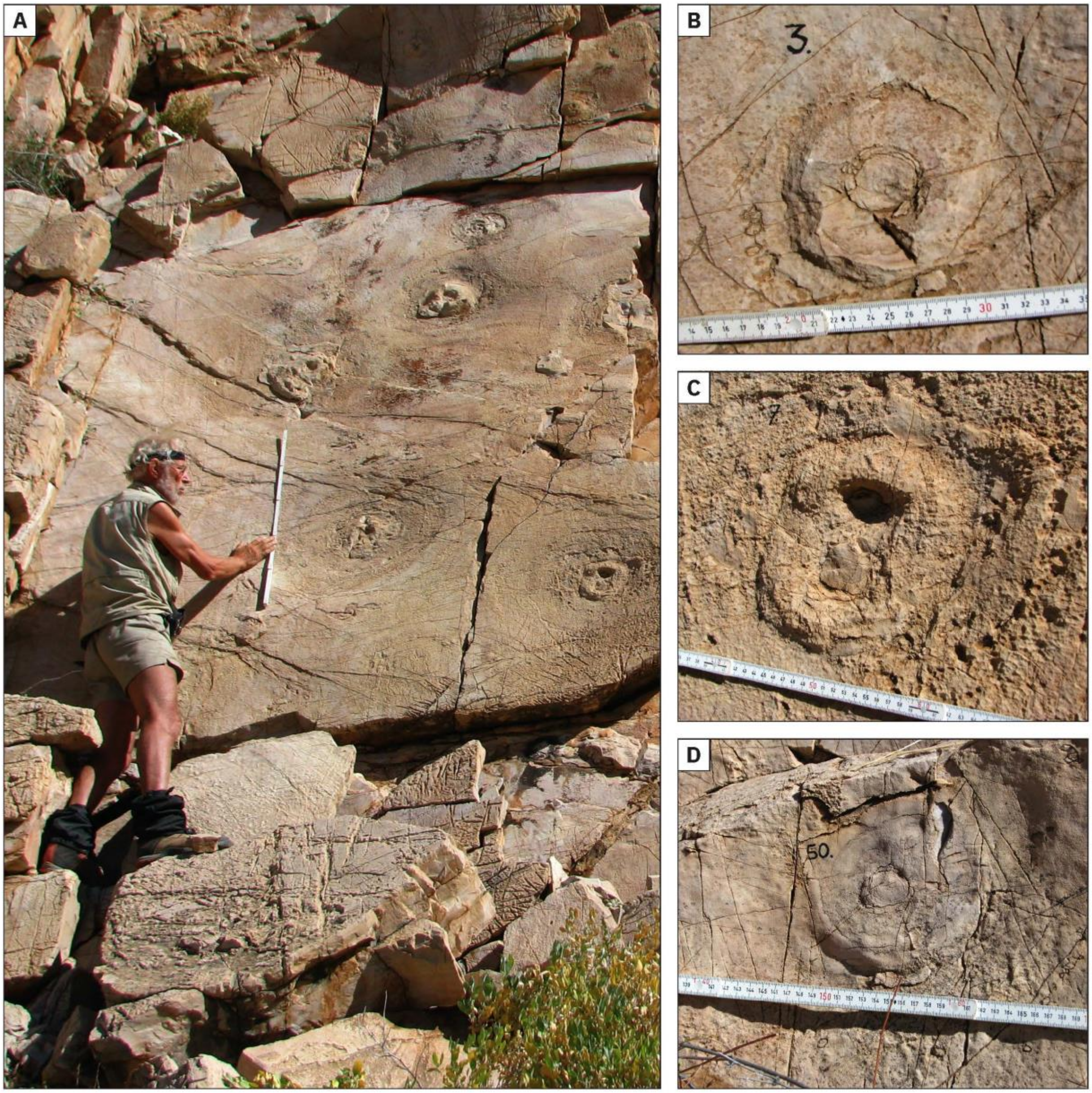
A
B
3.
C
7
D
50.

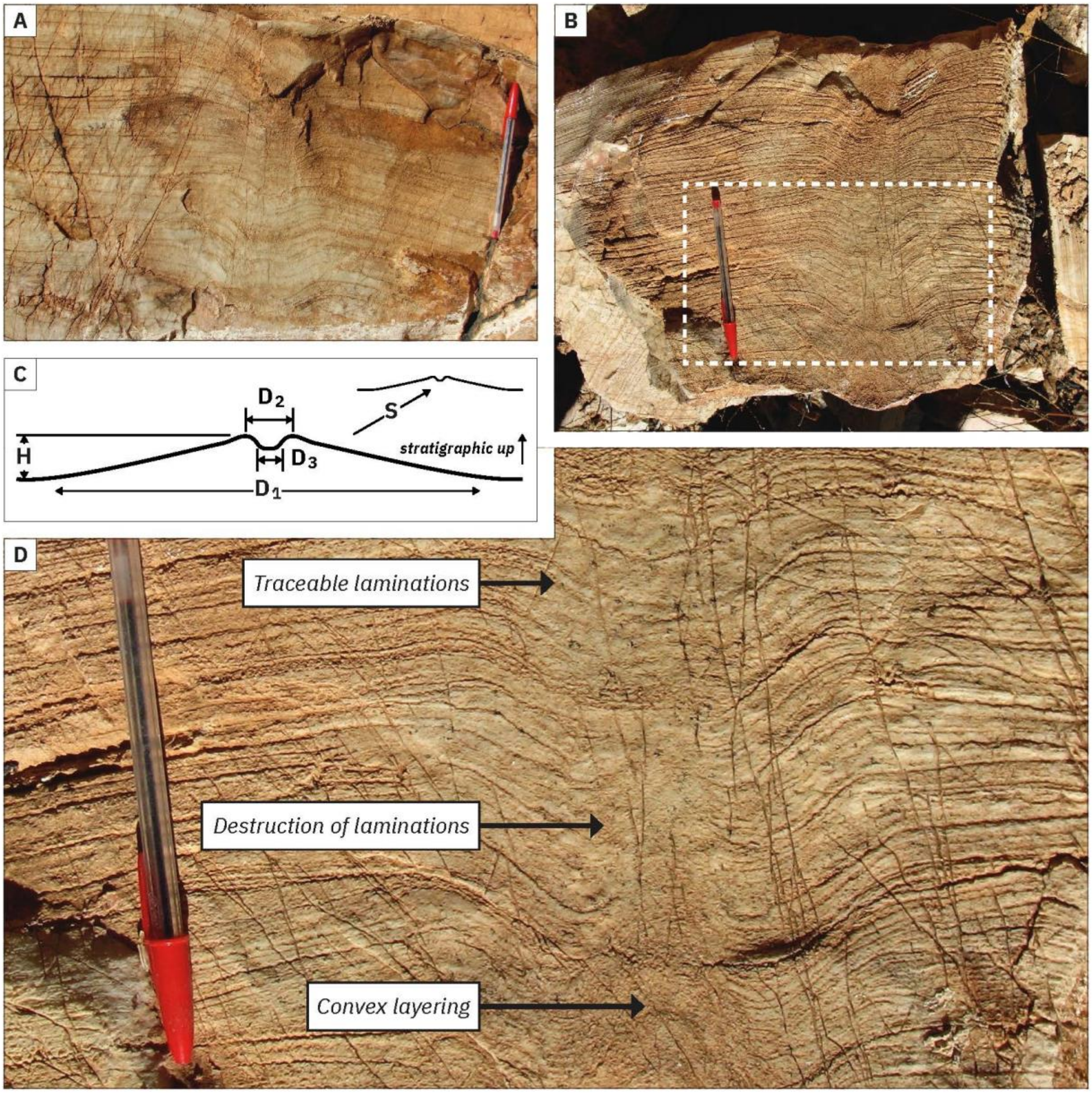
A
B
C
D₂
S
H
D₃
stratigraphic up
D₁
D
Traceable laminations
Destruction of laminations
Convex layering

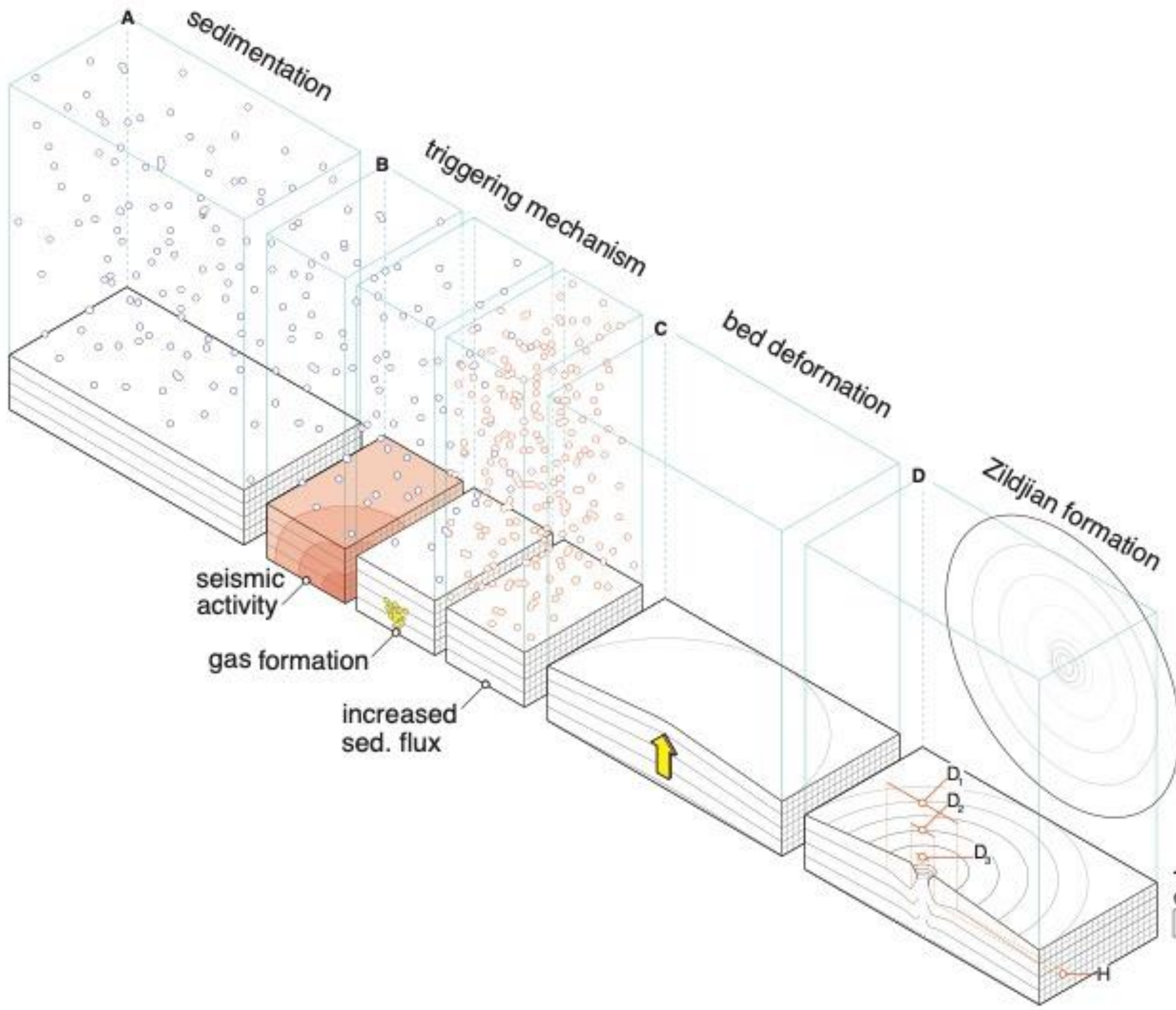

A
sedimentation
B
triggering mechanism
C
bed deformation
D
Zildjian formation
seismic
activity
gas formation
increased
sed. flux
D1
D2
D3
H
10
cm

564